J|A|C|S
ARTICLES
Published on Web 06/12/2003

Oxygen Adsorption on Hydrated Gold Cluster Anions: Experiment and Theory

William T. Wallace,* Richard B. Wyrwas, Robert L. Whetten, Roland Mitrić,† and Vlasta Bonačić-Koutecký†

Contribution from the School of Chemistry and Biochemistry and School of Physics, Georgia Institute of Technology, Atlanta GA, 30332-0400, and Institut für Chemie, Humboldt Universität zu Berlin, Brook-Taylor-Strasse 2, D-12489 Berlin, Germany

Received February 27, 2003; E-mail: wallace@chemistry.gatech.edu

Abstract: The discovery that supported gold clusters act as highly efficient catalysts for low-temperature oxidation reactions has led to a great deal of work aimed at understanding the origins of the catalytic activity. Several studies have shown that the presence of trace moisture is required for the catalysts to function. Using near-atmospheric pressure flow reactor techniques, we have studied humidity and temperature effects on the reactivity of gas-phase gold cluster anions with O_2. Near room temperature, the humid source produces abundant gold-hydroxy cluster anions, Au_NOH^-, and these have a reversed O_2 adsorption activity: Nonreactive bare gold clusters become active when in the form Au_NOH^-, while active bare clusters are inactive when $-$OH is bound. The binding energies for the stable structures obtained from density functional calculations confirm fully these findings. Moreover, the theory provides evidence that electron-transfer induced by the binding of a OH group enhances the reactivity toward molecular oxygen for odd anionic gold clusters and suppresses the reactivity for the even ones. The temperature dependence of O_2 addition to Au_3OH^- and Au_4^- indicates deviations from equilibrium control at temperatures below room temperature. The effects of humidity on gold cluster adsorption activity support the conclusion drawn for the mechanism of O_2 adsorption on "dry" gold cluster anions and provides insight into the possible role of water in the enhanced activity of supported gold cluster catalysts.

I. Introduction

Supported gold catalysts for air purification function well even in humid environments; indeed, trace levels of moisture are considered essential in order for the optimal activity of the catalysts to be achieved.[1,2] One proposal is that the dissociation of oxygen is necessary for the reaction to occur and that the presence of water aids in this dissociation.[3] However, it is also possible that water's role is to maintain an appropriate termination of the oxide support. As the nature of the actual working catalysts remains a challenge to characterization, an understanding of the activity of selected gas-phase gold clusters toward reactants of interest (O_2, CO, etc.) needs to be achieved, in the presence of H_2O, to separate the contributions to the catalytic activity of the gold clusters and the support material. The present experimental−theoretical report takes a first step in this direction, by exploring the adsorption of O_2 on the predominant forms of gold-hydrate anions.

The reactions of O_2 with gas-phase gold cluster anions have been described in detail in preceding reports.[4−8] At room temperature, all previous experimental studies have found that O_2 binds to Au_N^- in an even−odd manner, with odd-N clusters showing no activity toward O_2 adsorption, while the even-N clusters (except for $N = 10$ and 16) show a variety of relative reactivities and saturate at one molecule adsorbed.[7] This adsorption activity correlates well with the measured electron affinities of Au_N^- [9] and was interpreted within a simple frontier orbital picture. In this explanation, the adsorption occurs via electron transfer from the cluster to the O_2 π^* orbital. For those clusters with an unpaired electron in their HOMO (even-N clusters, low electron affinities), this mechanism can yield strong binding (∼1 eV), but for those with a filled HOMO (odd-N clusters, high electron affinities), it is not accessible. This

† Humboldt Universität zu Berlin.

(1) Haruta, M.; Yamada, N.; Kobayashi, T.; et al. Gold catalysts prepared by coprecipitation for low-temperature oxidation of hydrogen and of carbon monoxide. *J. Catal*. **1989**, *115*, 301.
(2) Haruta, M.; Tsubota, S.; Kobayashi, T.; et al. Low-temperature oxidation of CO over gold supported on TiO_2, α-Fe_2O_3, and Co_3O_4. *J. Catal*. **1993**, *144*, 175.
(3) Boccuzzi, F.; Chiorino, A. FTIR study of CO oxidation on Au/TiO_2 at 90 K and room temperature. An insight into the nature of the reaction centers. *J. Phys. Chem. B* **2000**, *104*, 5414.
(4) Cox, D. M.; Brickman, R.; Creegan, K.; et al. Gold clusters: reactions and deuterium uptake. *Z. Phys. D* **1991**, *19*, 353.
(5) Cox, D. M.; Brickman, R.; Creegan, K. Studies of the chemical properties of size selected metal clusters: kinetics and saturation. *Mater. Res. Soc. Symp. Proc*. **1991**, *206*, 34.
(6) Lee, T. H.; Ervin, K. M. Reactions of copper group anions with oxygen and carbon monoxide. *J. Phys. Chem*. **1994**, *98*, 10023.
(7) Salisbury, B. E.; Wallace, W. T.; Whetten, R. L. Low-temperature activation of molecular oxygen by gold clusters: A stoichiometric process correlated to electron affinity. *Chem. Phys*. **2000**, *262*, 131.
(8) Hagen, J.; Socaciu, L. D.; Elijazyfer, M.; et al. Coadsorption of CO and O_2 on small free gold cluster anions at cryogenic temperatures: Model complexes for catalytic CO oxidation. *Phys. Chem. Chem. Phys*. **2002**, *4*, 1707.
(9) Taylor, K. J.; Pettiette-Hall, C. L.; Cheshnovsky, O.; et al. Ultraviolet photoelectron spectra of coinage metal clusters. *J. Chem. Phys*. **1992**, *96*, 3319.

 10.1021/ja034905z CCC: $25.00

selective activity, as well as the correlation with the measured electron affinities, was explained by the suggestion that O_2 remains adsorbed molecularly (intact) as a one-electron acceptor, i.e., as a superoxo (O_2^-) adsorbate. The gold cluster possesses paired electrons in its HOMO and is thus inactive toward secondary adsorption.

Several theoretical studies concerning the Au_N^-/O_2 reaction system have been presented recently using density functional theory (DFT) methods.[10−13] These studies are generally in agreement with experiment, with odd-*N* clusters showing much lower O_2 binding energies than even-*N* clusters. However, compared to the experimental dissociation binding-energy estimates, the theoretical binding energies for O_2 to the even-*N* clusters are systematically higher in the literature, and significant (∼0.5 eV) binding energies are even seen on the odd-*N* clusters.[12,13] Thomson and co-workers performed DFT calculations on the interaction of O_2 with Au_{9-11}^- and suggested that basis-set superposition error for the relatively small basis set used resulted in higher binding energies for O_2 on Au_{10}^-.[13] Recently, Mills et al. performed more accurate coupled cluster calculations on the interaction of O_2 with Au_2^- and Au_3^-.[15] These calculations showed that the previously calculated O_2 binding energies were indeed too high for Au_2^-,and addition of an O_2 molecule to Au_3^- became slightly unfavorable. However, the appropriate choice of functionals in the DFT procedure, in particular for the exchange part, and a sufficiently large AO basis set allows for an accurate description of binding energies of O_2 with metal clusters, as will be shown in this contribution.

A full CO oxidation cycle under low reactant coverage conditions has been predicted for the gold dimer anion, Au_2^-,[10] and CO oxidation now has been seen on gold cluster anions as small as Au_6^- in fast-flow reactor experiments.[16] However, the question of the role of moisture in enhancing the CO oxidation activity of the supported gold clusters has yet to be addressed in gas-phase studies. The presence of H_2O-derived adsorbates could significantly alter the O_2-adsorption activity and mechanism. Such coadsorption effects have already been reported for the $\{CO,O_2\}$ combination,[8,16] and our joint experimental and theoretical work here extends this to $\{H_2O,O_2\}$ coadsorption. In this case, an abundant anionic species has the composition Au_NOH^-. The strongly electron-withdrawing OH group causes the odd-*N* gold subunits to be reactive toward binding of molecular oxygen.

II. Experimental Methods

The experimental techniques used to study the adsorption properties of O_2 on hydrated gold clusters have been described previously,[7] so only a brief description will be given here. Charged gold clusters are formed and equilibrated by laser vaporization of a rotating and translating gold rod in a high-pressure helium/H_2O flow stream, produced using a pulsed valve with a stagnation pressure of approximately 3.5 bar. Prior to entering the stagnation region of the pulsed valve, the helium is bubbled through H_2O, thereby saturating the helium with the vapor pressure of water at room temperature (∼20 mbar). The clusters are then exposed to a gas pulse from a secondary pulsed valve containing a dilute reactant gas (approximately 20% O_2:He with a stagnation pressure of ∼2 bar), expand into vacuum, and are detected by time-of-flight mass spectrometry, using perpendicular pulsed extraction fields. With the addition of a cooling sleeve (and heater) to the reactor, the effects of temperature on the reaction can also be studied under a source temperature range of 220−330 K. A variety of products are detected and will be discussed below. The mass spectra are found to be stable for the duration of the experiments, and all peak intensities have been accounted for, to rule out the contribution of decomposition reactions. Results arising from the use of D_2O instead of H_2O in the source region are identical; therefore, H_2O will be used in further discussion. A view of the cluster source and points of gas entry are shown in Figure 1.

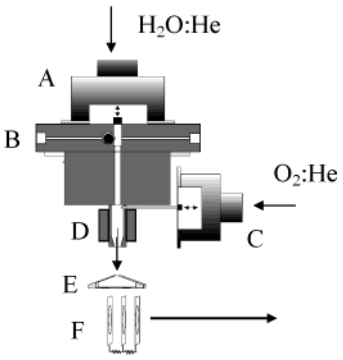

Figure 1. A view of the cluster source, reactor, and extraction region of the time-of-flight mass spectrometer adapted from ref 16. (A) The primary pulsed-gas valve, in which He bubbled through H_2O is used as a buffer gas in order to produce hydrated gold cluster anions. (B) The cluster source and expansion region, in which gold clusters are formed by laser vaporization of a gold rod and are allowed to react with the H_2O-seeded He buffer gas. The He also provides cluster cooling through third-body collisions. (C) The secondary pulsed-gas valve, by which a room-temperature mixture of ∼25% O_2:He can be added to (D) a 2.5 cm reaction zone. (E) A skimmer that collimates the beam of hydrated clusters and their reaction products for entry into (F) the perpendicular extraction region of a time-of-flight mass spectrometer.

III. Theoretical Methods and Accuracy

In this contribution, we use DFT method with Becke's hybrid three-parameter nonlocal exchange functional combined with the Lee−Yang−Parr gradient corrected correlation functional (B3LYP).[17] Calculations have been carried out with the 19-electron relativistic effective core potential (19-RECP) from the Stuttgart group for gold atom and the [9s7p5d1f]/[7s5p3d1f] AO basis set.[18] For oxygen and hydrogen atoms the 6-311 G(d,p) triple-ζ split valence basis set has been employed.[19]

To check the accuracy of the method, we compare calculated binding energies for small anionic gold clusters toward molecular oxygen with experimental data obtained from collision-induced dissociation (CID) studies of Lee and Ervin.[14] In the case of $Au_2^-{\cdot}O_2$ complex, the calculated binding energy of 1.06 eV is in excellent agreement with

(10) Häkkinen, H.; Landman, U. Gas-phase catalytic oxidation of CO by Au_2^-. *J. Am. Chem. Soc*. **2001**, *123*, 9704.
(11) Mills, G.; Gordon, M. S.; Metiu, H. The adsorption of molecular oxygen on neutral and negative Au_N clusters (N = 2−5). *Chem. Phys. Lett*. **2002**, *359*, 493.
(12) Mills, G.; Gordon, M. S.; Metiu, H. Oxygen adsorption on Au clusters and a rough Au(111) surface: The role of surface flatness, electron confinement, excess electrons and band gap. *J. Chem. Phys*. **2003**, *118*, 4198.
(13) Wells, D. H., Jr.; Delgass, W. N.; Thomson, K. T. Density functional theory investigation of gold cluster geometry and gas-phase reactivity with O_2. *J. Chem. Phys*. **2002**, *117*, 10597.
(14) Wallace, W. T.; Leavitt, A. J.; Whetten, R. L. Comment on: The adsorption of molecular oxygen on neutral and negative Au_N clusters (N = 2−5) [*Chem. Phys. Lett.* **2002**, *359*, 493]. *Chem. Phys. Lett*. **2003**, *368*, 774.
(15) Varganov, S. A.; Olson, R. M.; Gordon, M. S.; et al. Oxygen adsorption on Au clusters: Reply to a comment by W. T. Wallace, A. J. Leavitt, and R. L. Whetten. *Chem. Phys. Lett*. **2003**, *368*, 778.
(16) Wallace, W. T.; Whetten, R. L. Coadsorption of CO and O_2 on selected gold clusters: evidence for efficient room-temperature CO_2 generation. *J. Am. Chem. Soc*. **2002**, *124*, 7499.
(17) Becke, A. D. Density-functional exchange-energy approximation with correct asymptotic behavior. *Phys. Rev. A* **1988**, *38*, 3098; Becke, A. D. Density-functional thermochemistry. III. The role of exact exchange. *J. Chem. Phys.* **1993**, *98*, 5648. Lee, C.; Yang, W.; Parr, R. G. Development of the Colle−Salvetti correlation-energy formula into a functional of the electron density. *Phys. Rev. B* **1988**, *37*, 785.

the CID dissociation threshold value of 1.01 ± 0.14 eV. For $Au_4^-{\cdot}O_2$, a dissociation threshold of 0.74 eV, which includes the height of the barrier, is also in acceptable agreement with the CID result of 0.91 ± 0.14 eV, while the calculated binding energy has the value of 0.64 eV. The latter is also in agreement with experimentally estimated binding energy of 0.5 eV for $Au_4^-{\cdot}O_2$ (discussed below). As expected, for $Au_3^-{\cdot}O_2$ a binding energy of only 0.015 eV has been calculated, while the complex $Au_5^-{\cdot}O_2$ is not bound by −0.06 eV. This is consistent with the fact that these species have not been seen in experiments.[4−8] From the comparisons made with experiments, we conclude that the proper treatment of the exchange part of the density functional combined with the accurate basis set is needed for reliable description of the bonding between gold and oxygen. In this case, DFT calculations yield results of comparable accuracy as the coupled cluster method, in contrast to the statements recently published.[15] All the structures reported in this work have been fully optimized using a gradient-based minimization method, and the character of the stationary points has been checked by performing vibrational analysis. To study the electron transfer from the gold clusters to the oxygen, the natural bonding orbitals (NBO) analysis has been carried out.

IV. Results

(A) Hydrated Gold Cluster Anions ($Au_N{\cdot}OH^-$). Gold cluster anions in the size regime of 2−11 atoms have been produced using the methods described above in order to determine the effects of the presence of water on the adsorption activity of the clusters. Figure 2(bottom frame) shows a mass spectrum obtained for Au_3^- and Au_4^- species when ^2H_2O-seeded He buffer gas is used in the cluster source and the secondary (reactant) pulse is offset temporally from the main pulse. In addition to bare gold cluster anions, Au_N^-, several other species are obtained by this method, namely products corresponding to the formula $Au_N(OH)_{0-2}(H_2O)_{0-2}^-$. While the Au_NOH^- product seems to be the only strongly bound (non-displaceable) species, the present results are insufficient to determine unequivocally whether there are other favored hydration compositions.

The structural and electronic properties of the Au_NOH^- clusters ($N = 2-5$) have been systematically investigated using the theoretical methods described above. The optimized structures are shown in Figure 3 and the properties are summarized in Table 1. In all cases, the OH group is bound at a peripheral

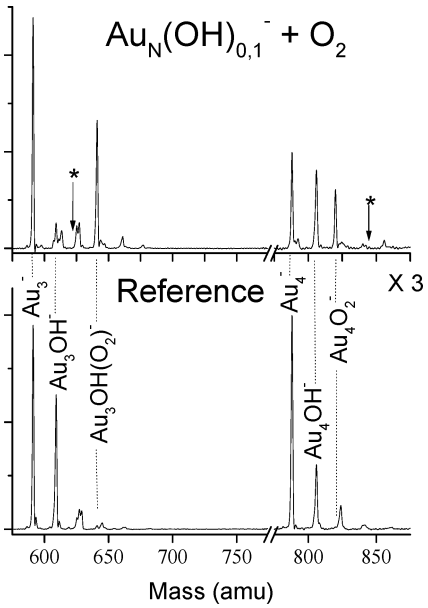

Figure 2. (Bottom) Mass spectrum of negatively charged gold clusters, Au_N^-, and various hydrates of the form $Au_N(OH)_{0,1,2}(H_2O)_{0,1,2}^-$, generated by adding H_2O into the buffer gas of the cluster source and the secondary gas pulse is temporally offset from the main (cluster) pulse (no reactant gas added). (Top) Mass spectrum obtained when the secondary gas pulse containing ~20% O_2:He is temporally overlapped with the main pulse. In addition to the depletion of the Au_4^- peak and Au_3OH^-, peaks appear at 32 amu higher mass, corresponding to O_2 adsorption.

position as found previously for bonding of the O_2 molecule on small anionic gold clusters.[11] However, consistent with the greater reactivity of the OH group compared to the O_2 molecule, the OH group is considerably stronger bound to the gold clusters. In general, the binding energies of complexes with the OH group and with molecular oxygen exhibit even−odd oscillations, but the absolute values are much higher for those with the OH group (cf. top frame of Figure 4). As a consequence, the anionic OH^- complexes with an odd number of Au atoms also become stable and have been detected experimentally. The complexes with even numbers of Au atoms are of course particularly stable. In the case of $Au_2^-{\cdot}OH$ species, the binding energy is −3.16 eV and a significant amount of electron transfer from the gold subunit to the OH group takes place, as can be seen from calculated natural bonding orbital (NBO) charges in Table 1. The binding energy for the O_2 molecule to the Au_2^- dimer is significantly lower, with a value of 1.06 eV, than in the case of the OH group.

Since the Au_3^- cluster has an even number of electrons, it is expected that the binding energy toward O_2 and OH group will be much lower. While the complex with O_2 is not bound, $Au_3^-{\cdot}OH$ is very stable, with an energy of 1.84 eV. The structures of the two lowest isomers with almost degenerate energies are shown in Figure 3. In the lowest energy isomer the OH group is bound at the peripheral atom of the almost linear structure, while in the second isomer the OH group is bound to the triangular gold subunit. Weaker bonding in $Au_3^-{\cdot}OH$ is also reflected in a significantly smaller amount of electron transfer to oxygen than in the case of $Au_2^-{\cdot}OH$, showing that the charge remains mainly localized on the Au_3 subunit in the former case.

In the stable structure of the $Au_4^-{\cdot}OH$ complex, the gold subunit assumes a T-form and the OH group is bound to a gold

(18) Andrae, D.; Haeussermann, U.; Dolg, M.; et al. Energy-adjusted ab initio pseudopotentials for the 2nd-row and 3rd-row transition-elements—Molecular test for Ag_2, Au_2 and RuH, OsH. *Theor. Chim. Acta* **1990**, *77*, 123. Gilb, S.; Weis, P.; Furche, F.; et al. Structures of small gold cluster cations (Au_n^+, n < 14): Ion mobility measurements versus density functional calculations. *J. Chem. Phys.* **2002**, *116*, 4094.
(19) McLean, A. D.; Chandler, G. S. Contracted Gaussian basis sets for molecular calculations. I. Second row atoms, $Z = 11-18$. *J. Chem. Phys.* **1980**, *72*, 5639; Krishnan, R.; Binkley, J. S.; Seeger, R.; et al. Self-consistent molecular orbital methods. XX. A basis set for correlated wave functions. *J. Chem. Phys.* **1980**, *72*, 650.
(20) Jackschath, C.; Rabin, I.; Schulze, W. Electron impact ionization potentials of gold and silver clusters M_n, n ≤ 22. *Ber. Bunsen-Ges. Phys. Chem.* **1992**, *96*, 1200.
(21) Cheeseman, M. A.; Eyler, J. R. Ionization potentials and reactivity of coinage metal clusters. *J. Phys. Chem.* **1992**, *96*, 1082.
(22) Bauschlicher, C. W.; Langhoff, S. R.; Partridge, H. Theoretical study of the homonuclear tetramers and pentamers of the group IB metals (Cu, Ag, Au). *J. Chem. Phys.* **1990**, *93*, 8133.
(23) Häberlen, O. D.; Chung, S.-C.; Stener, M.; et al. From clusters to bulk: a relativistic density functional investigation on a series of gold clusters Au_n, n = 6,...,147. *J. Chem. Phys.* **1997**, *106*, 5189.
(24) Bonačić-Koutecký, V.; Burda, J.; Mitrić, R.; Ge, M.; Zampella, G.; Fantucci, P. Density functional study of structural and electronic properties of bimetallic silver−gold clusters: Comparison with pure gold and silver clusters. *J. Chem. Phys.* **2002**, *117*, 3120.
(25) Mitrić, R.; Bürgel, C.; Burda, J.; Bonačić-Koutecký, V.; Fantucci, P. Structural properties and reactivity of bimetallic silver−gold clusters. *Eur. Phys. J. D*, in press.

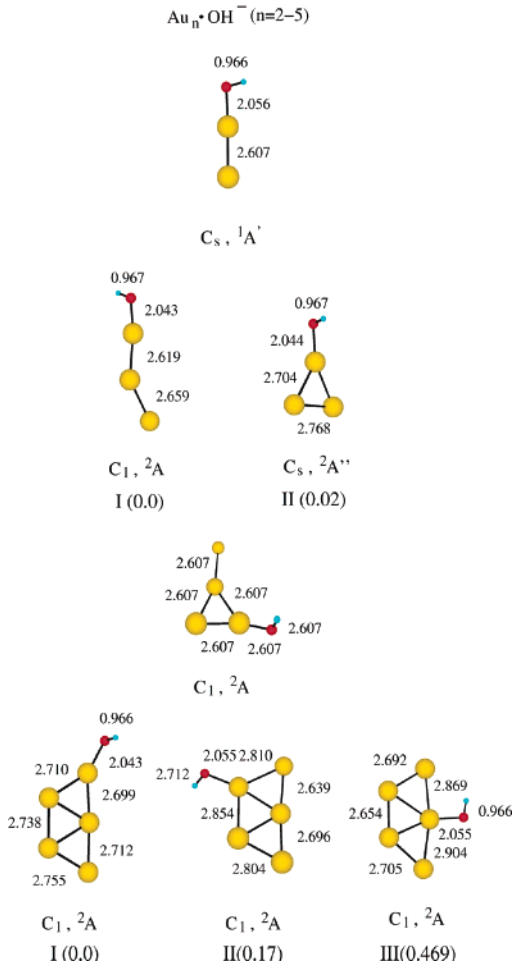

Figure 3. Optimized structures of Au_NOH^- complexes ($N = 2-5$). For the Au_5 system, ΔE values (in eV) for different isomers are given in parentheses. Oxygen and hydrogen atoms are labeled by large red and small blue circles, respectively. Isomers corresponding to the local minima whose relative energies are less than 1 eV with respect to the most stable structure are shown.

Table 1. Ground-State Energies and Properties of Optimized Au_NOH^- ($N = 2-5$) Clusters Obtained with the B3LYP Method

Au_NOH^-, $N = 2$–5	symm (state)	energy, au	ΔE,[a] eV	E_b,[b] eV	NBO charge Au_N	NBO charge OH
Au_2OH^-	C_s ($^1A'$)	−347.514 326		3.16	−0.35	−0.65
Au_3OH^-(I)	C_1 (^2A)	−483.314 557		1.84	−0.63	−0.37
Au_3OH^-(II)	C_s ($^2A''$)	−483.313 657	−0.02			
Au_4OH^-	C_1 (^1A)	−619.158 765		3.00	−0.38	−0.62
Au_5OH^-(I)	C_1 (^1A)	−754.961 885		2.30	−0.65	−0.35
Au_5OH^-(II)	C_1 (^1A)	−754.955 443	−0.17			
Au_5OH^-(III)	C_1 (^1A)	−754.944 645	−0.47			
$Au_2O_2^-$	C_1 (^2A)	−422.054 480		1.06		
$Au_3O_2^-$	C_1 (^3A)	−557.869 781		0.015		
$Au_4O_2^-$	C_1 (^2A)	−693.694 330		0.64		
$Au_5O_2^-$	C_{2v} ($^3A_2$)	−829.497 109		−0.06		

[a] Energy difference with respect to the most stable structure. [b] Binding energy for the Au_NOH^- complexes is defined by $E_b = E(Au_NOH^-) - E(Au_N^-) - E(OH)$, and for the $Au_NO_2^-$ complexes as $E_b = E(Au_NO_2^-) - E(Au_N^-) - E(O_2)$.

atom that is part of the triangular subunit. The binding energy of 3.16 eV is close to that of Au_2^-·OH, and the negative charge is located at the OH group as well. At the same time, the binding energy toward O_2 is considerably lower (0.64 eV) due to a lower electron affinity than in the case of OH.

The most stable structure of Au_5^-·OH complex has a planar trapezoidal Au_5 subunit with the OH group placed at the

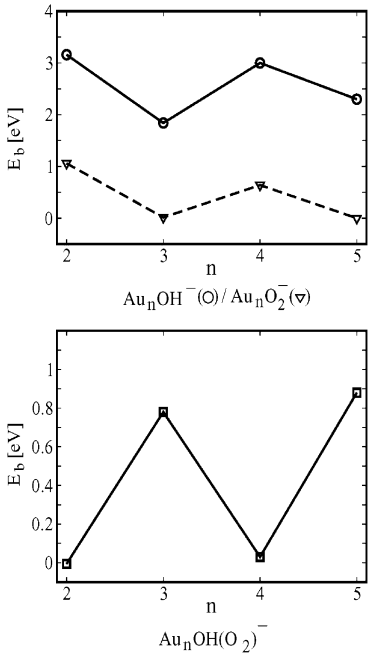

Figure 4. (Top) Binding energies of O_2 (triangles) and OH (circles) on Au_N^- clusters ($N = 2-5$). For stable structures of Au_NOH^- complexes cf. Figure 3. Au_N^-·O_2 complexes have common structures with those published previously.[11] (Bottom) O_2 adsorption energies on Au_NOH^- cluster complexes ($N = 2-5$). For stable structures of $Au_NOH(O_2)^-$ cf. Figure 7.

peripheral position, which is most convenient to withdraw the charge from the two coordinated Au atoms. In fact, in other higher energy isomers shown in Figure 3, the OH group is attached to the three- and four-coordinated gold atom, respectively. The binding energy of Au_5^-·OH is larger than in the case of Au_3^-·OH, and electron transfer is again considerably reduced with respect to the complexes with an even number of gold atoms. In contrast, Au_5·$^-O_2$ is not bound (−0.06 eV). A comparison of the binding energies for Au_N·OH^- and Au_N·$(O_2)^-$ complexes as a function of the cluster size is shown in the top frame of Figure 4.

(B) Adsorption of Molecular Oxygen on Hydrated Gold Cluster Anions ($Au_NOH(O_2)^-$). When a secondary gas pulse containing dilute O_2:He is overlapped with the main (cluster) pulse in the experiments, mass spectra of the type shown in Figure 2 (top frame) are obtained. As can be seen, overlap of the pulses results in the depletion of several peaks in the mass spectrum, as well as the growth of new peaks at 32 amu higher mass. For the even-N clusters, O_2 addition proceeds as expected, with the adsorption of a single molecule on the bare cluster, as in

$$Au^-_{N(\text{even})} + O_2 \rightarrow Au_{N(\text{even})}O_2^- \qquad (1)$$

For the odd-N clusters, however, rather surprising results occur. As no O_2 adsorption has been seen on these clusters in the past and no or extremely weak binding has been calculated (cf. Figure 4 and Table 1.), it is not surprising to find that no complexes of the type $Au_{N(\text{odd})}O_2^-$ are present in the mass spectrum. However, on odd-N clusters of the type $Au_{N(\text{odd})}OH^-$, adsorption of a single O_2 molecule is found, according to the reaction

$$Au_{N(\text{odd})}OH^- + O_2 \rightarrow Au_{N(\text{odd})}OH(O_2)^- \qquad (1')$$

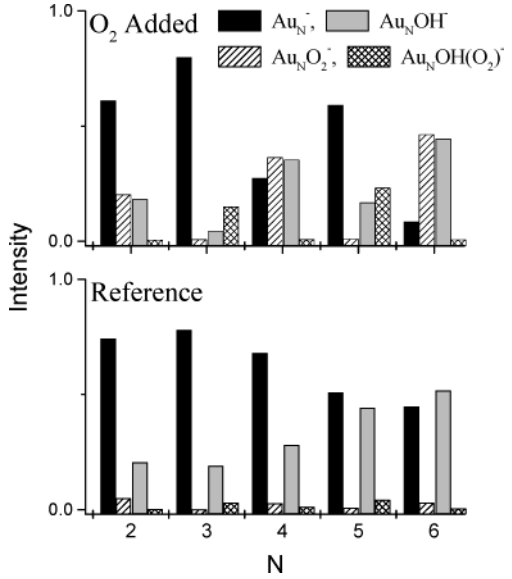

Figure 5. Bar graph representation of the normalized cluster intensities of Au_N^- and Au_NOH^- when the secondary gas pulse is temporally offset (bottom) and overlapped (top) with the main cluster pulse. This shows that reaction (1′) is the only significant process for O_2 addition to odd-*N*, clusters while the presence of an −OH group on the even-*N* clusters causes them to lose all activity for O_2 addition.

In contrast, on $Au_{N(even)}OH^-$ clusters, no O_2 adsorption activity is detected. The normalized intensities of these major peaks are plotted in Figure 5 for $N = 2-6$, both when the O_2 pulse is temporally offset from the main pulse (bottom frame) and overlapped (top frame). This figure clearly shows that reaction 1′ is the only significant process for O_2 addition to odd-*N* clusters, while even-*N* clusters simply add O_2 to the bare clusters, as in reaction 1. An extension to $N = 11$ confirms that this pattern applies up to at least the $N = 11$ cluster. Further studies are underway on the larger gold cluster anions, and a full report is forthcoming.

The size-dependent adsorption activity of the different cluster species can be quantitatively described by some simple calculations. Using the normalized cluster intensities shown in Figure 5 (top frame), the relative reactivities, or extent of reaction, of the various clusters at a fixed O_2 concentration can be calculated by

$$\frac{[Au_NO_2^-]}{[Au_NO_2^-] + [Au_N^-]} \qquad (2)$$

for the bare clusters or by

$$\frac{[Au_NOH(O_2)^-]}{[Au_NOH(O_2)^-] + [Au_NOH^-]} \qquad (2')$$

for the hydrated clusters. The extents of reaction for different O_2 concentrations are plotted in Figure 6 according to eq 2 in the bottom frame and eq 2′ in the top frame. Upper bounds for the reactivity of the even-*N* Au_NOH^- clusters and odd-*N* Au_N^- clusters have been plotted using the magnitude of the baseline noise as an upper limit for the corresponding O_2 peak intensity. Just as in Figure 5, this figure readily indicates the even−odd activity of the $Au_NOH^- + O_2$ reaction system. What is also interesting to note is the extremely high reactivity of Au_3OH^-

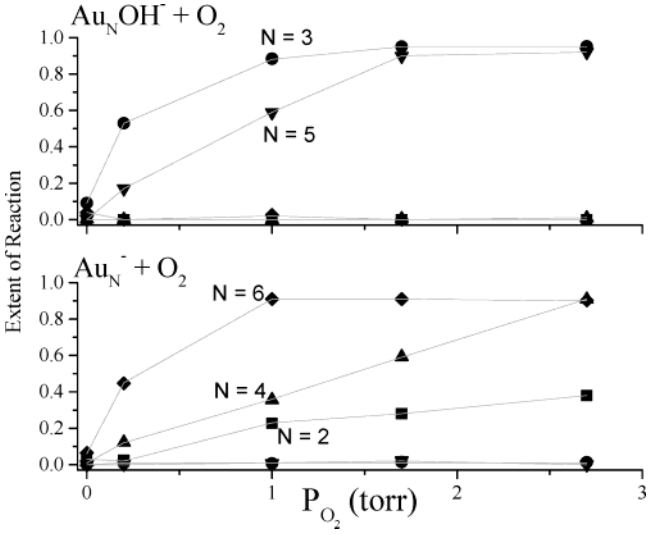

Figure 6. Cluster-size dependence of the extent of reaction, as defined in eq 2 (bottom) and eq 2′ (top) for different partial pressures of O_2 in the reactor. These pressures are calculated from the overall pressure in the reactor (∼100 Torr), the difference in average pressure achieved when the secondary valve fires, as well as the difference in pulse length, and the known dilutions of O_2:He. The extents of reaction for odd-*N* Au_N^- clusters and even-*N* Au_NOH^- clusters are upper limits.

at lower O_2 partial pressures, which approaches (and even exceeds) the activity of Au_6^-, the most active bare gold cluster, at lower O_2 partial pressures.

To investigate the reactivity of Au_NOH^- complexes toward molecular oxygen, structures of the $Au_NOH(O_2)^-$ complexes (Figure 7) and their stabilities (Table 2) have been determined (cf. also Figure 4**)**. Theory confirms the experimental finding that the affinity toward O_2 is reversed compared to the reactivity of pure anionic gold clusters.

The $Au_2OH(O_2)^-$ complex is not bound, in contrast to Au_2^-, which strongly binds O_2 (cf. Figure 4). The NBO analysis shows that there is almost no electron transfer from the Au_2 subunit to the O_2 molecule. In contrast, Au_3OH^- binds O_2 strongly, and a significant amount of electron transfer from the Au_3 subunit takes place (cf. Table 2). The O_2 molecule is bound as a superoxide subunit in the $Au_3OH(O_2)^-$ complex, as reflected in the NBO charge and the O−O bond length, which is significantly longer than for molecular oxygen. The $Au_3OH(O_2)^-$ stable complex has a triangular structure with OH and O_2 bound at the neighboring Au atoms. In contrast, the complex of $Au_4OH(O_2)^-$ is again only very weakly bound and has a triplet ground state. There is no significant electron transfer from the gold subunit to O_2 and, correspondingly, the O−O bond is shorter.

In the stable structure of $Au_5OH(O_2)^-$, the O_2 molecule is bound in a peroxo-like form, bridging two gold atoms of the trapezoidal Au_5 subunit. The binding energy has the value of 0.88 eV and is slightly higher than for $Au_3OH(O_2)^-$ (0.78 eV). Again, stronger interaction with the Au_5 subunit is reflected in the electron transfer and in the O−O bond length. The trapezoidal Au_5 subunit is slightly positively charged, due to the complete electron transfer to the OH and O_2 subunits. In other higher energy isomers of $Au_5OH(O_2)^-$, O_2 is bound to a single Au atom, and therefore, the withdrawing of the electron from the gold subunit is lower than in the case of the lowest energy isomer.

Table 2. Ground State Energies and Properties of Optimized $Au_NOH(O_2)^-$ ($N = 2-5$) Clusters Obtained with the B3LYP Method

$Au_NOH(O_2)^-$, $N = 2-5$	symm (state)	energy, au	ΔE, eV	E_b, eV	NBO charge Au_N	NBO charge OH	NBO charge O_2
$Au_2OH(O_2)^-$	C_1 (^{3}A)	−497.883 874		−0.006	−0.195	−0.638	−0.167
$Au_3OH(O_2)^-$ (I)	C_1 (^{2}A)	−633.713 091		0.78	0.154	−0.310	−0.844
$Au_4OH(O_2)^-$	C_1 (^{3}A)	−769.529 684		0.03	−0.174	−0.606	−0.220
$Au_5OH(O_2)^-$ (I)	C_1 (^{2}A)	−905.364 643		0.88	0.114	−0.322	−0.835
$Au_5OH(O_2)^-$ (II)	C_1 (^{1}A)	−905.351 662	0.353				
$Au_5OH(O_2)^-$ (III)	C_1 (^{1}A)	−905.350 389	0.388				
$Au_5OH(O_2)^-$ (IV)	C_1 (^{1}A)	−905.341 137	0.640				

[a] Energy difference with respect to the most stable structure. [b] Binding energy for the $Au_NOH(O_2)^-$ complexes is defined by $E_b = E(Au_NOH(O_2^-)) - E(Au_NOH^-) - E(O_2)$.

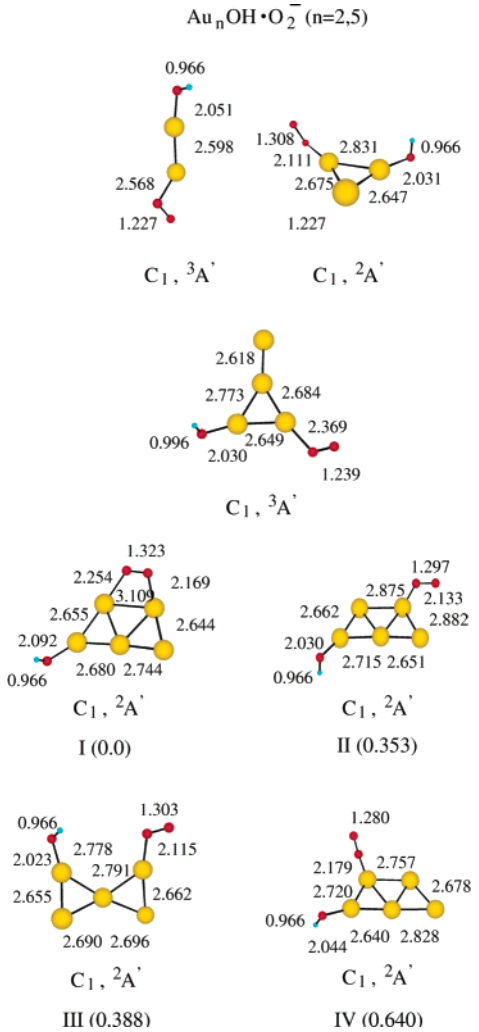

Figure 7. Optimized structures of $Au_NOH(O_2)^-$ complexes ($N = 2-5$). For the Au_5 system, ΔE values (in eV) for different isomers are given in parentheses. Oxygen and hydrogen atoms are labeled by large red and small blue circles, respectively. Isomers corresponding to the local minima whose relative energies are less than 1 eV with respect to the most stable structure are shown.

(C) Determination of Binding Energies from the Temperature Dependence of the Apparent Equilibrium Constant. In an attempt to determine the binding energies of O_2 on the reactive gold cluster species and to facilitate a comparison with the theoretical values of binding energies, the temperature of the reaction system has been varied between the range of 258 and 318 K. Using this method, the binding energies can be determined using the equation

$$\Delta \ln K = \frac{-\Delta_r H}{R}\Delta\frac{1}{T} + \frac{\Delta S}{R} \tag{3}$$

in which $\Delta_r H$ is the binding energy of O_2 on the cluster, ΔS is the entropy of adsorption, and the relative equilibrium constant, K, at a constant O_2 concentration is defined by

$$K = \frac{[Au_NO_2^-]}{P_{O_2}[Au_N^-]} \tag{4}$$

for even-N clusters. For odd-N clusters, Au_N^- would be replaced by Au_NOH^- and $Au_NO_2^-$ would be replaced by $Au_NOH(O_2)^-$. Representative plots of ln K vs $1/T$ obtained from eq 3 are shown in Figure 8 for Au_3OH^- and Au_4^- for two different partial pressures of O_2. Linear fits for the high temperature data are also shown in the figure. For simple adsorption behavior, the relative equilibrium constant should continue to increase with decreasing temperature. As is readily apparent from Figure 8, this is not the case for the two species shown. In the case of Au_4^-, a linear fit can only be made for temperatures above room temperature (rt, ~298 K), the slope of which gives an approximate O_2 binding energy (ΔH_r) of 0.53 ± 0.01 eV, which is lower than the value determined by Lee and Ervin in collision-induced dissociation experiments by approximately 0.5 eV.[14] At temperatures lower than room temperature, however, the value of the apparent equilibrium constant becomes much less steep. At this stage of the analysis, this activity is not understood, and further studies are underway to gain a better understanding of the low-temperature behavior of O_2 adsorption. Therefore, we have chosen to focus on the high-temperature activity (≥ rt) for these discussions.

The behavior of Au_3OH^- is also not simple. Up to temperatures just below room temperature, the value of the apparent equilibrium constant is actually *increasing*, suggesting that an effective energy barrier must be overcome for O_2 to bind to the cluster. Only beginning immediately below room temperature does the value of the apparent equilibrium constant begin to decrease with increasing temperature. From a linear fit to this data, a binding energy of approximately 0.47 ± 0.05 eV can be obtained. While these binding energies are significantly different from those calculated here and measured experimentally (described in ref 14), the plots still give important qualitative information, namely, that at lower temperatures kinetics may play an important role and an equilibrium treatment of these systems may not be applicable. Further studies are underway to determine if this behavior holds for larger N sizes of Au_N^- and Au_NOH^-.

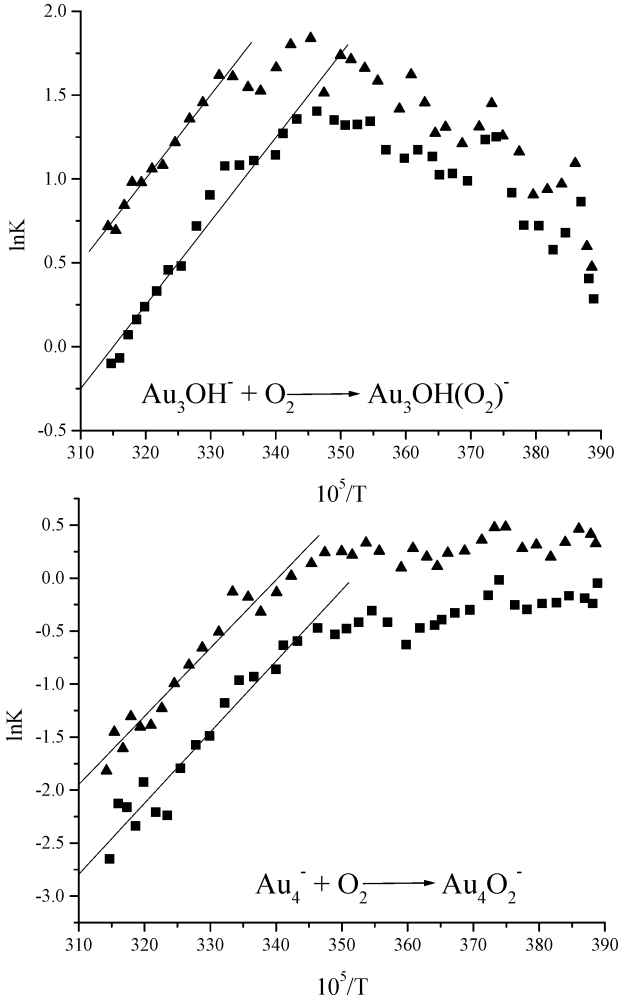

Figure 8. Plots of the gas phase temperature dependence of the apparent equilibria $Au_3OH^- + O_2$ (top) and $Au_4^- + O_2$ (bottom) obtained from eq 3 for two reactant concentrations. The plots correspond to ln *K* vs 1/*T*. At higher temperatures, the lines are a linear fit to the data, yielding the binding energies described in the text.

V. Discussion

The easiest (and perhaps most pleasing) explanation for the selective activity of the Au_NOH^- species toward O_2 adsorption draws on a comparison to the activity of the bare Au_N^- clusters. As described above, with the high electron affinity of OH (~1.8 eV), the electron transfer from the even-*N* clusters to OH becomes highly favorable and causes transfer from the odd-*N* clusters to become stable. In such a case, the electronic structure of the gold clusters reverses from the situation seen for bare clusters, i.e., the bare, odd-*N* Au_N^- clusters have no unpaired electrons, while the odd-*N* Au_NOH^- clusters now have an unpaired electron on the gold cluster. In this case, in an attempt to once again pair electrons, the open-shell cluster complexes could adsorb O_2 as a one-electron acceptor.

An analysis of the experimental and theoretical results provided here support this bonding mechanism for the Au_3OH^- cluster and is described as follows: First, the OH group binds to a closed shell Au_3^- cluster. Due to the high electron affinity of the OH group, electron transfer from Au_3^- to the OH takes place, resulting in an almost neutral Au_3 subunit, which then, due to its open shell structure, strongly binds O_2. In the resulting complex, the gold subunit has a positive charge and negative charge is mainly localized at the O_2 superoxide subunit.

Table 3. Experimental and Theoretical Values for Au_N ($N = 2-6$) Ionization Potentials

	IP (eV)				
ref	Au_2	Au_3	Au_4	Au_5	Au_6
20[a]	9.50	7.50	8.60	8.00	8.80
21[b]	9.16 ± 0.10	7.27 ± 0.15		7.61 ± 0.20	
22[c]	9.41	7.06	7.98	7.46	
23[d]					7.60
24,25[e]	9.63	7.30	8.09	7.68	8.37

[a] Experimental; upper limits for IP. [b] Experimental; no value reported for Au_4 or Au_6. [c] Theoretical; no value reported for Au_6. [d] Theoretical; Au_6 is the smallest cluster reported. [e] Theoretical.

With this mechanism in mind, a greater understanding of this system could be provided by further studies of the activity of the neutral gold clusters, Au_N. In this case, subsequent O_2 adsorption depends on the ionization potential (IP) of the neutral cluster species. Several experimental and theoretical values of Au_N IPs are collected in Table 3. An analysis of these values provides additional insight into the observed extents of reaction. While the absolute values of the cluster IPs are somewhat different, the *overall trends* are consistent. Beginning with Au_2, a strong even−odd oscillation in cluster IP is seen (as with the measured extents of reaction), with the even-*N* clusters having significantly higher IPs than the odd-*N* clusters. Within the odd-*N* clusters studied, the IP value for Au_5 is higher than that for Au_3, which is consistent with the lower extent of reaction for Au_5 (cf. Figure 6).

While a separate understanding of the adsorption properties of {O_2, CO, etc.} is important to gain an understanding of the CO oxidation activity of free anionic gold clusters, it is their coadsorption properties that may play the largest role. Studies using the methods described for the current experiments were recently used to study the coadsorption of {CO, O_2} on small gold cluster anions, Au_N^- ($N \leq 10$).[16] Those experiments showed that, in many cases, CO and O_2 adsorb cooperatively on Au_N^-. Instead of lowering the probability of subsequent adsorption, the presence of a preadsorbate increases the ability of the cluster to bind an incoming molecule. This activity holds when either CO or O_2 is the preadsorbate. Very recent work by the group of Wöste also provided exciting results on the reactions of $Au_{2,3}^-$.[8] Using a temperature-controlled ion trap, they found that only Au_2^- showed activity toward O_2 adsorption over the temperature range of 100−350 K. Under 250 K, however, *when CO is preadsorbed*, Au_3^- shows the addition of both one and two O_2 molecules, in the form $Au_3(CO)(O_2)^-$ and $Au_3(CO)(O_2)_2^-$. Only under conditions in which CO was preadsorbed, and at low temperatures, was O_2 adsorption able to be seen on this odd-*N* cluster anion, reinforcing the concept of cooperative coadsorption. The present results show that the coadsorption properties of {H_2O, O_2} on Au_N^- are equally interesting and suggest the need for further studies on the {H_2O, CO} and {H_2O, O_2, CO} coadsorption systems.

Acknowledgment. W.T.W, R.B.W., and R.L.W. would like to acknowledge the National Science Foundation for financial support and would like to thank Prof. Andrew J. Leavitt for technical assistance with the variable temperature experiments. R. M. gratefully acknowledges the financial support by the DAAD.

JA034905Z